Journal of Magnetic Resonance 198 (2009) 41–48

Contents lists available at ScienceDirect

Journal of Magnetic Resonance

journal homepage: www.elsevier.com/locate/jmr

Robust and efficient spin-locked symmetry-based double-quantum homonuclear dipolar recoupling for probing ^{1}H–^{1}H proximity in the solid-state

B. Hu [a], Q. Wang [a,b,c], O. Lafon [a], J. Trébosc [a], F. Deng [b,*], J.P. Amoureux [a,*]

[a] UCCS, CNRS-8181, Lille University, Fr-59652, Villeneuve d'Ascq Cedex, France
[b] State Key Laboratory of Magnetic Resonance and Atomic and Molecular Physics, Wuhan Center for Magnetic Resonance, Wuhan Institute of Physics and Mathematics, Chinese Academy of Sciences, Wuhan 430071, China
[c] Graduate School of the Chinese Academy of Sciences, Beijing, China

ARTICLE INFO

Article history:
Received 15 October 2008
Revised 19 December 2008
Available online 13 January 2009

Keywords:
Solid-state NMR
Spin-1/2 nuclei
Fast MAS
Double-quanta spectroscopy

ABSTRACT

We report a novel symmetry-based method, using inversion elements bracketed by spin locks, for exciting double-quantum (DQ) coherences between spin-1/2 nuclei, such as protons. Compared to previous DQ-recoupling techniques, this new pulse sequence requires moderate rf field, even at ultra-fast MAS speeds. Furthermore, it is easy to implement and it displays higher robustness to both chemical shift anisotropy and to spreads in resonance frequencies. These advances greatly facilitate the observation of ^{1}H–^{1}H proximities at high fields and high MAS frequencies.

1. Introduction

Many applications of solid-state Nuclear Magnetic Resonance (NMR) to molecular structure determination are based on dipole–dipole couplings between nuclei since they encode important information on the spatial proximity of atoms through their dependence on the inverse cube of the inter-nuclear distance. A wide variety of dipolar recoupling methods exist for the exploitation of dipole–dipole couplings in the presence of magic-angle spinning (MAS). A particularly important class of recoupling techniques restores the dipole–dipole coupling between spins of the same isotopic type [1–4]. Such homonuclear dipolar recoupling methods may be classified according to the rotational spin rank of the recoupled dipolar Hamiltonian. In particular, double-quantum (DQ) homonuclear recoupling has a number of important applications, including suppression of signals from isolated spins [5], two-dimensional DQ–SQ correlation spectroscopy [6–10], high-order multiple-quantum excitation in solids [11], and the estimation of inter-nuclear distances [12] and torsional angles [13].

The focus here is on DQ homonuclear recoupling of ^{1}H nuclei, which are increasingly exploited in the solid state because of the high sensitivity and the high natural abundance of this isotope [8–10]. Furthermore, the efficiency of current homonuclear decoupling sequences precludes the use of small ^{1}H–^{1}H J couplings (typically less than 10 Hz, whereas the ^{1}H line-widths span hundreds of Hz) to create DQ coherences (DQC).

The ^{1}H DQ homonuclear recoupling sequences that have been mostly used so far are the BAck to BAck (BABA) [14,15], and the (CN_n^ν, RN_n^ν) symmetry-based [16,17] schemes. For slow spinning speeds ($\nu_R \leqslant$ 15–20 kHz), POST-C7 [18,19], $C9_1^4$ [9], $R14_2^6$ [20] and SR26 [21] sequences can be used. However, the required rf-field amplitude is proportional to the spinning speed for symmetry-based sequences, e.g. $\nu_1 = 9\nu_R$ for $C9_1^4$, which means that these sequences are hardly usable at fast MAS speeds, due to probe rf-limitations.

BABA [14,15,22] sequence has been to date the method of choice for ^{1}H DQ recoupling at fast or ultra-fast MAS frequencies ($\nu_R >$ 30 kHz). The original BABA sequence [14], denoted BABA-1 in this article, spans over one rotor period and consists of two evolution periods bracketed by two 90° pulses (see Fig. 1b). BABA-1 has a short cycle time but it is very sensitive to resonance offsets and chemical shift anisotropy (CSA). Partial compensation of these unwanted interactions can be achieved by super-cycling pulse phases over two rotor periods, as shown in Fig. 1c. This variant, denoted BABA-2, display a higher robustness with respect to resonance offsets than BABA-1. However, the performance of BABA sequences is relatively poor in cases of large chemical shift differences. This precludes the observation of DQ–SQ correlations between ^{1}H nuclei at high static magnetic field (see Fig. 7). In addition, in between the pulses, the proton magnetization is submitted to losses due to flip–flop terms (T_2'), which can lead to a large signal decrease. Last, in the case of strong ^{1}H–^{1}H interactions

* Corresponding authors. Fax: +33 3 20 43 68 14.
E-mail addresses: dengf@wipm.ac.cn (F. Deng), jean-paul.amoureux@univ-lille1.fr (J.P. Amoureux).

1090-7807/$ - see front matter © 2009 Elsevier Inc. All rights reserved.
doi:10.1016/j.jmr.2009.01.002

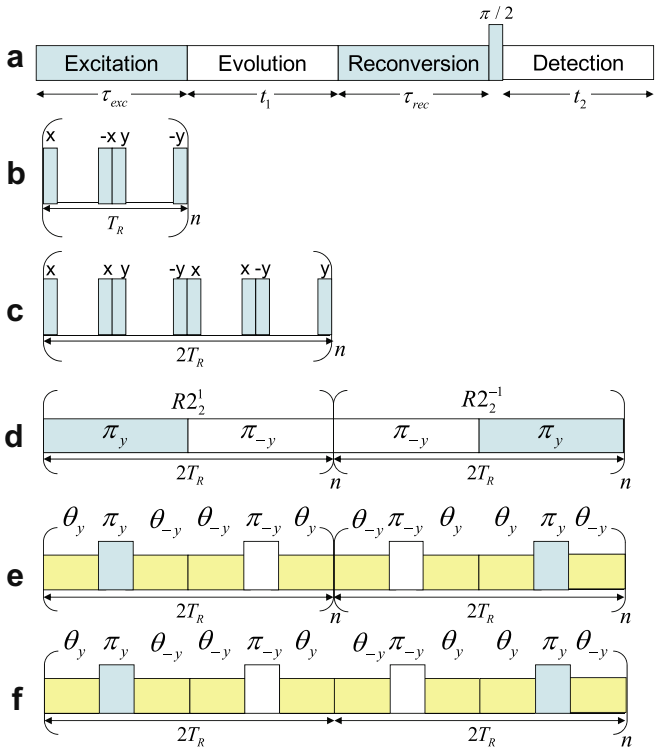

Fig. 1. (a) General scheme of DQ–SQ experiments. Following are pulse sequences for DQ ↔ SQ excitation or reconversion: (b) BABA-1, (c) BABA-2, (d) super-cycled version of $R2^1_2(\pi)$, (e) SPIP and (f) SPIP′. BABA sequences use $\pi/2$ pulses. The basic SPIP or SPIP′ element lasts one T_R and consists in one π pulse sandwiched by the two spin-lock parts (θ_y and θ_{-y}). The super-cycling can be performed in two ways: (e) SPIP consists of n blocks of $2T_R$ each belonging to $R2^1_2$ symmetry class followed by n blocks of $2T_R$ each, belonging to $R2_2^{-1}$ symmetry class and (f) SPIP′ consists of n blocks of $4T_R$ each belonging to $R2^1_2R2_2^{-1}$. In the case of not γ-encoded sequences (BABA, $R2^1_2$, or SPIP), the evolution time t_1 must be an integer multiple of rotor periods.

and slow or moderate spinning speeds, the magnitude of dipole–dipole interactions recoupled by both BABA sequences is too large compared to their cycle times, T_R or $2T_R$. In other words, the build up of DQC is too fast compared to the minimal sampling period of the recoupling intervals. This result in abrupt variations in the double-quantum efficiency as function of the recoupling intervals and in a reduction in the double-quantum-filtered signal amplitude (see Fig. 2).

To solve these three problem, we propose in this article a new robust and efficient pulse sequence that does not need large rf power and can be used for broadband DQ NMR spectroscopy in rotating solids, at both moderate and fast MAS speeds.

2. Theory and simulations

An ideal DQ recoupling sequence should have the following characteristics: (i) the double quantum efficiency should be as large as possible; (ii) the sequence should be usable at high spinning frequencies, in order to ensure high spectral resolution and sensitivity and to minimize spinning sidebands generated by CSA; (iii) the sequence should have minimal dependence on isotropic and anisotropic shielding; (iv) the rf field requirement should be compatible with usual probe specifications; and (v) the magnitude of recoupled dipole–dipole interactions should be much lower than the maximal sampling frequency of the recoupling intervals.

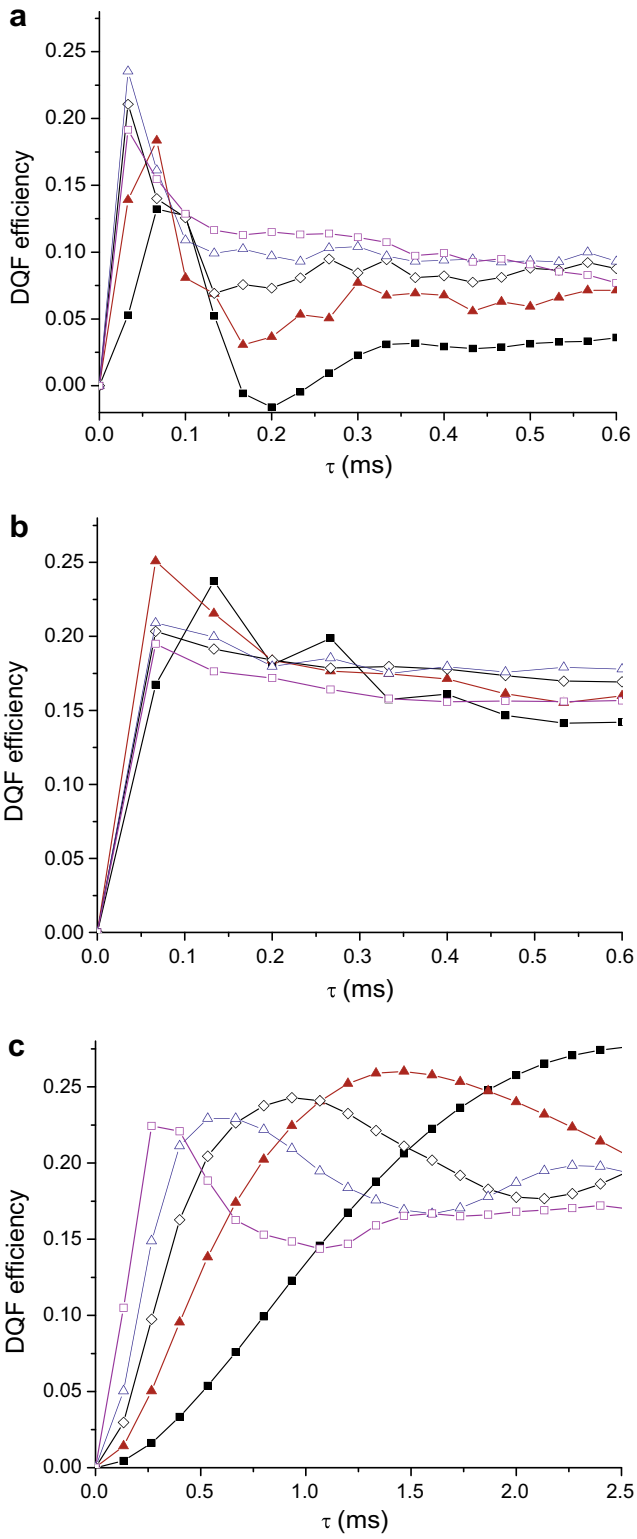

Fig. 2. Calculated DQF efficiency as function of τ, for DQF experiments with different DQ recoupling schemes: (a) BABA-1 ($\tau = nT_R$), (b) BABA-2 ($\tau = 2nT_R$), (c) SPIP ($\tau = 4nT_R$). The spin system consists of two protons with the same chemical shift and the dipolar coupling constant between them is b_{12} = 5 (■),9 (▲),13 (◇),17 (Δ),25 (□) kHz. The recoupling sequences were applied on-resonance at ν_R = 30 kHz. For BABA-1 and BABA-2, the rf nutation frequency is ν_1 = 100 kHz, while for SPIP it is equal to $\nu_{1\pi}$ = 67.5 kHz for the central π pulse, and ν_{1SL} = 62 kHz for the spin-locking pulses. CSA of the two spins is equal to 4.4 kHz (η = 0.8) and 11.2 kHz (η = 0).

2.1. Symmetry-based recoupling

The design of recoupling pulse sequences is facilitated by the use of symmetry theory [16,17]. The new pulse sequence is originated from the $R2_2^1(\pi)$ symmetry-based sequence [16,23,24], which is composed of a series of π-pulses, each occupying one whole rotor period with the phase of adjacent pulses being shifted by π. One of its super-cycled version is represented in Fig. 1d. Considering solely the homonuclear dipolar coupling between two like spins j and k, the $R2_2^1(\pi)$ sequence, based on these continuous π-pulses, corresponds to the following zero-order average Hamiltonian [23]:

$$\bar{H}_{R2_2^1} = b_{jk} f(\beta,\gamma)\{I_j^+ I_k^- + I_j^- I_k^+ - 4I_{jz}I_{kz} + I_j^+ I_k^+ + I_j^- I_k^-\} \quad (1)$$

where b_{jk} is the dipolar coupling constant and $f(\beta,\gamma) = 3\sin 2\beta \cos\gamma/(16\sqrt{2})$ is a function of the Euler angles, β and γ, randomly distributed in a powder, relating the inter-nuclear vector to the rotor frame. Consequently, the magnitude of the recoupled interaction depends on the Euler angle γ and the $R2_2^1$ sequence is not γ-encoded and hence the evolution time t_1 must be an integer multiple of rotor periods (T_R). In this respect, the $R2_2^1$ recoupling method is similar to BABA schemes. Moreover, it can be seen in Eq. (1) that $R2_2^1$ sequence can excite both zero- and double-quantum coherences from longitudinal polarization. However, only the DQ part of this Hamiltonian is involved in DQ recoupling.

2.2. Basic element

Besides the homonuclear dipolar coupling terms, the zero-order average Hamiltonian corresponding to $RM_M^{M/2}$ sequences also contains isotropic chemical shift (offset) and CSA terms having spin quantum numbers $\{\lambda,\mu\} = \{1,\pm1\}$. The sensitivity to offset irradiation can be decreased by increasing the rf amplitude. To that end, the original basic element, a soft continuous π pulse, was replaced by a strong rotor-synchronized π pulse (see Fig. 1e), as previously done in HORROR recoupling [25]. Furthermore, it is well-known that spin-locking allows decreasing the effect of offset if the spin-lock field is sufficient. Therefore, two compensated spin-lock periods were added, one on each side of the central π pulse. Finally, In other words, the basic inversion element of the $R2_2^1$ sequence we used corresponds to a $\theta_y\pi_y\theta_{-y}$ composite pulse that provides a rotation of π about the rotating-frame y-axis. The resulting pulse sequence is denoted $R2_2^1(\theta_y\pi_y\theta_{-y})$. As $R2_2^1(\pi)$ and $R2_2^1(\theta_y\pi_y\theta_{-y})$ sequences belong to the same symmetry class, the symmetry allowed and forbidden terms are the same but differ in magnitude. In the case of $R2_2^1(\theta_y\pi_y\theta_{-y})$ sequence, the scaling factor depends on the π pulse length as well as the θ value.

2.3. Super-cycle

The unwanted offset and CSA terms can be further suppressed in the zero-order average Hamiltonian by applying a super-cycle. In the same way as for DQ recoupling between quadrupolar nuclei (Fig. 1d) [23,26], we have chosen a super-cycle constructed by applying an overall phase shift of π from the middle of the recoupling sequence (see Fig. 1e). For simplicity reasons, this sequence has been called Sandwiched PI Pulse (SPIP). The 2Q phase super-cycle eliminates the offset and CSA terms in the zero-order average Hamiltonian. As already observed in the case of quadrupolar nuclei [23], SPIP recoupling scheme leads to better performance than the sequence displayed in Fig. 1f, hereafter denoted SPIP′. The zero-order average Hamiltonian of SPIP contains ZQ and DQ homonuclear dipolar couplings as well as homonuclear J coupling. Contrary to the two previously published methods [23,26], the $R2_2^1$-based irradiation was not sandwiched by two bracketing $\pi/2$ pulses. Indeed, bracketing the sequence described in Fig. 1e leads to a doubling of the double-quantum part of the zero-order average Hamiltonian Eq. (1) [23]. This doubling has two negative effects: (i) it divides by two the optimum contact times, which may be a limitation when spinning slowly, and (ii) it increases largely the sensitivity to offset irradiation (see Fig. 5).

2.4. 1D DQ-filtered experiment and 2D DQ–SQ spectroscopy

The performances of SPIP sequence were tested by incorporating such recoupling in one-dimensional (1D) DQ-filtered experiments as well as 2D DQ–SQ sequence.

The 1D DQ-filtered sequence corresponds to the scheme of Fig. 1a when $t_1 = 0$. A DQ recoupling sequence is applied for an interval τ_{exc} in order to transform the longitudinal magnetization into DQC. A second recoupling period of duration τ_{rec} followed by $\pi/2$ pulse transforms the DQCs into observable transverse magnetization. Signals passing through DQCs are selected by a four-step phase cycle of the pulses used for exciting or reconverting the DQCs. This is called double-quantum filtering (DQF) [10]. The build-up of DQCs may be estimated by acquiring DQ-filtered NMR signals as function of the intervals τ_{exc} and τ_{rec}. Different protocols can be used [10,27,28]. In the following, we will only describe the results obtained with the symmetric protocol, i.e. the two intervals τ_{exc} and τ_{rec} are both incremented but kept equal to each other: $\tau = \tau_{exc} = \tau_{rec}$. Nevertheless SPIP recoupling can also be used in DQF experiments with unequal recoupling times.

Although DQF experiments are useful to test the efficiency and the robustness of the SPIP recoupling, they only allow determining whether a spin species is subject to dipole–dipole couplings, but the identity of the other spins involved in the couplings remains unknown. In order to identify the two spin species forming a dipolar-coupled pair, the DQF experiment has to be extended to a 2D version. A commonly employed approach is 2D DQ–SQ spectroscopy. This sequence derives from 1D DQF experiment by inserting an incremented time period t_1 between the excitation and reconversion recoupling intervals, as depicted in Fig. 1a. Hence, the evolution of DQCs in t_1 is correlated with that of single-quantum coherences (SQC) in t_2 and the resulting 2D spectra display DQ–SQ correlations. In a 2D DQ–SQ spectrum, the spins that are alike and close in space result in diagonal peaks with a slope of 2, and a pair of unlike spins results in a pair of cross-peaks at the sum of the two SQ frequencies along the DQ dimension. For instance, two unlike spins with SQ frequencies of ν_A and ν_B will give rise to two cross-peaks at a DQ frequency of $\nu_A + \nu_B$. The intensity of the cross-peaks is an indication of the strength of the dipolar coupling between the spins and in turn of the inter-nuclear distance. Applications of ^{1}H DQ spectroscopy in various systems have proved the utility of this approach [6–8].

2.5. Numerical simulations

In preparation for the experiments, we performed simulations with the SIMPSON software [29], and the powder averaging was performed using 320 crystallites following the REPULSION algorithm [30]. Spinning speed, chemical shifts, dipolar couplings and rf and static fields are specified in the figure captions. In Figs. 2–5, the vertical axes show the calculated DQF efficiencies defined as the ratio of the integral of DQ filtered spectra to the integral of 1D spectrum obtained after $\pi/2$-pulse excitation [31]. For simulations shown in Figs. 2–4, the spin system consists of two protons with the same chemical shift. In these cases, the recoupling sequences were applied on-resonance.

Fig. 2 compares the build-up of DQF efficiencies as a function of the excitation/reconversion time τ for three DQ recoupling schemes (BABA-1, BABA-2, and SPIP) incorporated in a DQF experiment at

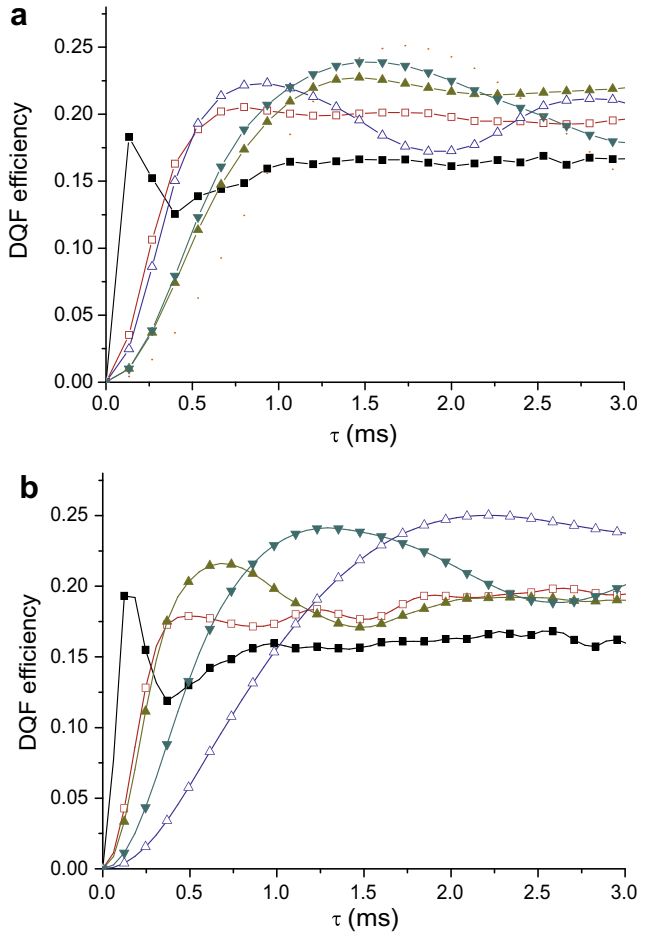

Fig. 3. Calculated DQF efficiency as function of τ for DQF experiment with SPIP recoupling at two MAS speeds. Different rf nutation frequencies of the π-pulse were employed: (a) $\nu_R = 30$ kHz and $\nu_{1\pi} = 45$ (■), 60 (□), 75 (▲), 90 (Δ), and 105 (▼) kHz; (b) $\nu_R = 65$ kHz and $\nu_{1\pi} = 90$ (■), 120 (□), 150 (▲), 180 (Δ), and 210 (▼) kHz. The spin system consists of two protons with the same chemical shift and the dipolar coupling constant between them is $b_{12} = 11$ kHz. The recoupling sequence is applied on-resonance and the rf nutation frequency for the spin locking pulses is fixed to $\nu_{1SL} = 0.7\nu_{1\pi}$. CSA of the two spins is equal to 4.4 kHz ($\eta = 0.8$) and 11.2 kHz ($\eta = 0$).

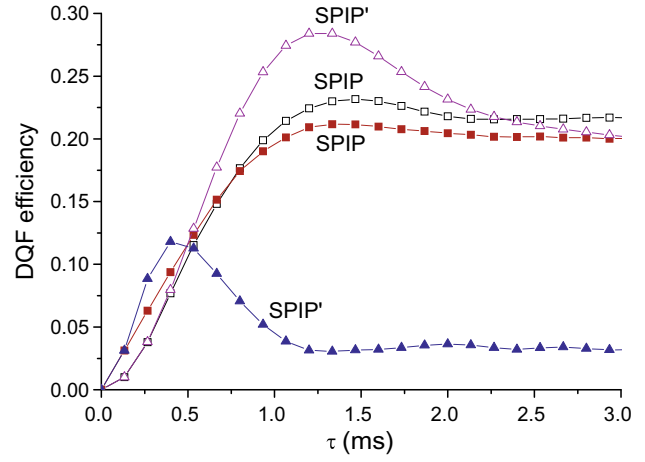

Fig. 4. Calculated intensity of an on-resonance two spin-system versus τ, with $b_{12} = 11$ kHz, $\nu_R = 30$ kHz. $\nu_{1\pi} = 75$ kHz, $\nu_{1SL} = 52.5$ kHz. The sequences are either that of Fig. 1e (SPIP: squares) or that of Fig. 1f (SPIP′: triangles). CSA has been introduced in the calculations: either 8 kHz (open) or 24 kHz (solid).

$\nu_R = 30$ kHz. The dipolar coupling constant between the two protons was varied from $b_{12} = 5$ to 25 kHz. It must be reminded that the τ values can only be multiples of 33 μs (T_R: BABA-1), 67 μs ($2T_R$: BABA-2), or 133 μs ($4T_R$: SPIP) (see Fig. 1). At this speed, the maximum BABA efficiencies (≈25%) are only accessible for moderate dipolar interactions: $b_{12} \approx 17$ kHz (BABA-1) or $b_{12} \approx 9$ kHz (BABA-2) (Fig. 2a and b). It must be noted that BABA-2 sequence appears more 'robust' than BABA-1 scheme, in the sense that the DQF efficiencies decrease more slowly than those of BABA-1 for recoupling times longer than the optimum value. Therefore, the efficiency of BABA-2 can be larger at slower spinning speeds than that of BABA-1. However, experimentally, this advantage of BABA-2 may be counterbalanced by larger T'_2 losses since the maxima in DQF efficiencies are reached for twice longer recoupling times in the case of BABA-2 as compared to BABA-1. On the contrary, we obtain the same optimum efficiency (≈25%), but for much longer recoupling times with SPIP sequence (Fig. 2c), which means an easy setting up, even with slow spinning speeds. Actually, this advantage is due to the small scaling factor of the homonuclear dipolar interaction when $\theta_y\pi_y\theta_{-y}$ pulse is used as basic element. Furthermore, as SPIP is a windowless sequence, the irreversible losses during the long recoupling times arise only from $T_{1\rho}$ losses, which are smaller than T'_2 losses affecting BABA experiments. It must be mentioned that SPIP is only weakly sensitive to CSA. The maximum efficiency of SPIP (≈25%), is much smaller than that accessible with γ-encoded sequences, such as POST-C7 (≈35%) [18,19]. However, it must be reminded that these sequences are not usable at fast MAS speeds ($\nu_R \geqslant$ 15–20 kHz), as opposed to SPIP.

In Fig. 3 we have represented the DQF efficiency as function of τ for several amplitudes $\nu_{1\pi}$ of the central π pulses in SPIP recoupling, and for two spinning speeds: $\nu_R = 30$ kHz (Fig. 3a) and 65 kHz (Fig. 3b). The maximum intensity first starts to increase with weak $\nu_{1\pi}$ values, and then becomes approximately constant as long as the π pulse amplitude is approximately at least twice the spinning speed.

In Fig. 4, we have represented the intensity of the spectra of the previous on-resonance two spin system with SPIP (Fig. 1e: two blocks lasting $2nT_R$ each) or SPIP′ (Fig. 1f: n blocks lasting $2T_R$ each). These simulations show that SPIP sequence (Fig. 1e) is much more efficient and much less CSA dependent than the SPIP′ variant

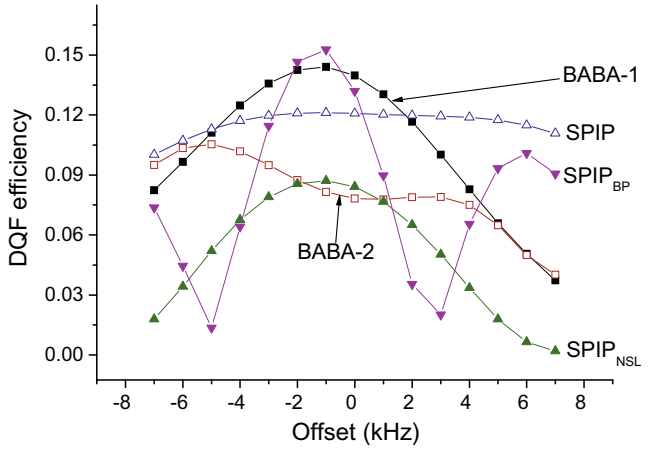

Fig. 5. Calculated intensity of nucleus 1 in a three spin-system versus offset of this nucleus. Five different homonuclear DQ recoupling sequences were compared at a MAS frequency $\nu_R = 30$ kHz: BABA-1 (■, $\tau = 33.3$ μs), BABA-2 (□, $\tau = 66.6$ μs), SPIP (Δ, $\tau = 933$ μs), SPIP$_{NSL}$ (▲, $\tau = 133$ μs) and SPIP$_{BP}$ (▼, $\tau = 533$ μs). The spin system parameters were as follows: the isotropic chemical shifts of nuclei two and three were at +2 and −3 kHz from that of nucleus 1 and the anisotropic chemical deshielding constant and CSA asymmetry parameters, δ_{aniso} (kHz)/η, were 4.4/0.8, 11.2/0.58, 0/0 for nuclei 1, 2, and 3, respectively. The dipolar coupling constants amongst the three spins were $b_{12} = 11$ kHz, $b_{13} = 6.63$ kHz, and $b_{23} = 6.75$ kHz.

described in Fig. 1f. At large magnetic fields, this is important for ^{1}H and critical for nuclei experiencing large CSA, such as ^{31}P. This better robustness of SPIP recoupling as compared to SPIP′ has been verified experimentally (not shown). Therefore, in the following, we will not consider the SPIP′ sequence described in Fig. 1f.

Fig. 5 shows the calculated dependence of DQF efficiency as function of resonance offset for five recoupling sequences, BABA-1, BABA-2, SPIP and two of its variants: with either no spin-lock periods ($SPIP_{NSL}$) or with two bracketing 90° pulses ($SPIP_{BP}$) as in references [23,26]. The simulations were performed for a spin system containing three protons and spinning at $\nu_R = 30$ kHz. It may be observed that BABA-1, $SPIP_{NSL}$ and especially $SPIP_{BP}$ are quite sensitive to offset effects as opposed to the two other methods. BABA-2 is more sensitive to offsets and less efficient than SPIP. The difference in sensitivity would increase when taking into account irreversible losses since they are more important for BABA-2 (T_2') than for SPIP ($T_{1\rho}$). It must also be noted that the SPIP recoupling time leading to maximal DQF efficiency are seven times much longer with the spin lock periods ($\tau^{opt} = 933$ μs) than without ($\tau^{opt} = 133$ μs). This means that the scaling factor is c.a. seven times smaller in the first case than in the second case due to the change of the basic elements.

3. Experimental results and discussion

We have tested the SPIP and BABA experiments on three different samples: L-histidine.HCl.H_2O, NaH_2PO_4 and a phosphate compound. The experiments on L-histidine·HCl·H_2O were performed on a narrow bore 18.8 T Bruker Avance-II spectrometer equipped with 3.2 mm MAS probe spinning at $\nu_R = 23.6$ kHz. Those on NaH_2PO_4 were performed on a wide bore 9.4 T Bruker Avance-II spectrometer equipped with a 2.5 mm MAS probe spinning at $\nu_R = 31.7$ kHz. Those on the phosphate sample were performed with the same previous two probes at both 9.4 and 18.8 T.

We have tested on L-histidine·HCl·H_2O, the optimum spin-lock amplitude ν_{1SL} that can be observed when fixing the π pulse amplitude to $\nu_{1\pi} = 71$ kHz (Fig. 6). This figure displays a large plateau, which means that the spin-lock value can remain quite moderate ($\nu_{1SL} \geqslant 35$ kHz). Actually, simulations performed with different $\nu_{1\pi}$ and ν_R values have shown that this plateau always starts at moderate rf-values: c.a. $\nu_{1SL} \geqslant 0.5\nu_{1\pi}$.

We have tested the offset sensitivity of L-histidine·HCl·H_2O for four different sequences: BABA-1 (Fig. 7a), BABA-2 (Fig. 7b), $SPIP_{NSL}$ (Fig. 7c) and SPIP (Fig. 7d). The experimental results confirm previous simulations concerning offset irradiations (Fig. 5): (i) BABA-1 is the most sensitive method to these effects, (ii) $SPIP_{NSL}$ and BABA-2 are less sensitive to offsets, but also less efficient on-resonance, and (iii) SPIP presents the great advantage of being insensitive to offsets and of providing a large efficiency identical that of BABA-1 on resonance.

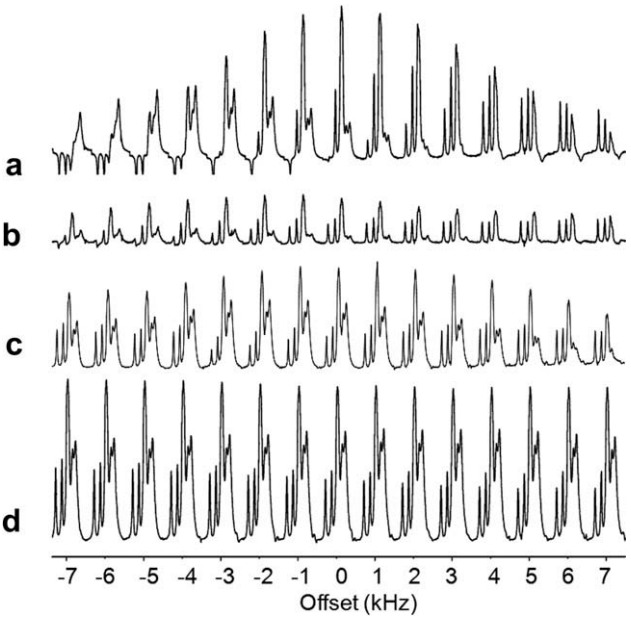

Fig. 7. Experimental ^{1}H DQF spectra of L-histidine·HCl·H_2O at 18.8 T and $\nu_R = 23.6$ kHz as function of the resonance offset of the H^N peak (see the assignment in Fig. 8b). Four different homonuclear DQ recoupling sequences were compared: (a) BABA-1 with $\nu_{1\pi} = 91$ kHz and $\tau = 42.4$ μs, (b) BABA-2 with $\nu_{1\pi} = 91$ kHz and $\tau = 84.8$ μs, (c) $SPIP_{NSL}$ with $\nu_{1\pi} = 71$ kHz and $\tau = 170.8$ μs, and (d) SPIP with $\nu_{1\pi} = 71$ kHz, $\nu_{1SL} = 59$ kHz, and $\tau = 169.5$ μs. Each recoupling sequence employed experimentally optimized excitation and reconversion intervals, τ, and nutation frequencies. Each spectrum was acquired with 32 scans and a recycle delay of 2 s. The experimental results confirm previous simulations concerning offset irradiations (Fig. 5): (i) BABA-1 is the most sensitive method to these effects, (ii) $SPIP_{NSL}$ and BABA-2 are less sensitive to offsets, but also less efficient on-resonance, and (iii) SPIP presents the great advantage of being insensitive to offsets and of providing a large efficiency identical to that of BABA-1 on resonance.

In Fig. 8, we have represented three DQ–SQ spectra of L-histidine.HCl.H_2O, recorded with BABA-1 (Fig. 8b), BABA-2 (Fig. 8c) and SPIP (Fig. 8d). By comparing the F2 projections of Fig. 8b–d,

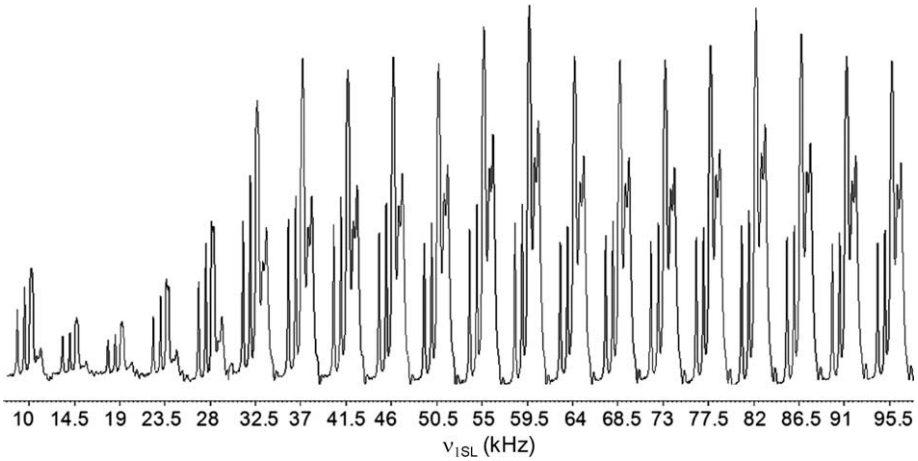

Fig. 6. Experimental ^{1}H DQF spectra of L-histidine·HCl·H_2O at 18.8 T and $\nu_R = 23.6$ kHz for the SPIP sequence (described in Fig. 1e) as function of the spin-lock nutation frequency, ν_{1SL}. The nutation frequency of the central π pulse was kept constant at $\nu_{1\pi} = 71$ kHz. Each spectrum was acquired with 32 scans and a recycle delay of 2 s. This figure displays a large plateau, which means that the spin-lock value can remain quite moderate: $\nu_{1SL} \geqslant 35$ kHz, or more generally $\nu_{1SL} \geqslant 0.5\nu_{1\pi}$.

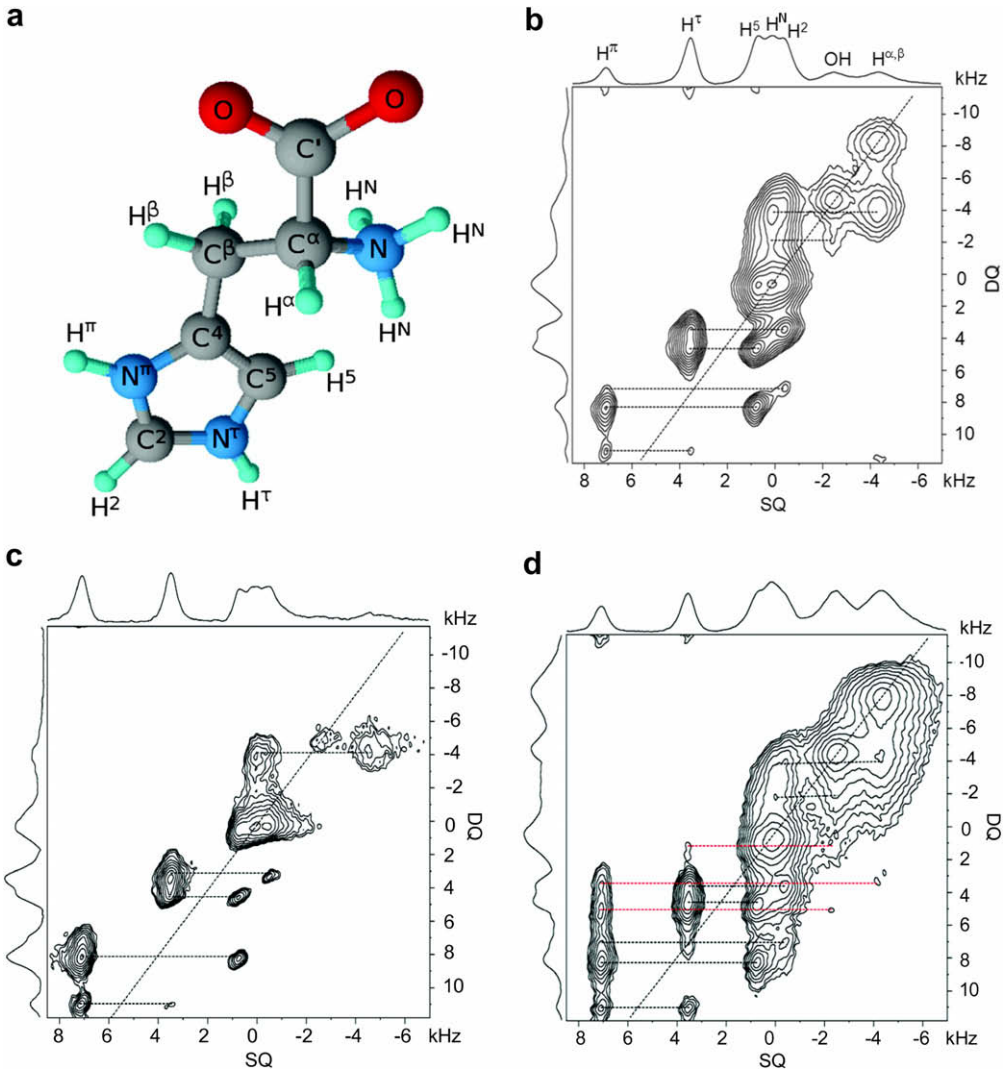

Fig. 8. L-histidine·HCl·H_2O. (a) Molecular structure with atom labelling matching IUPAC recommendations. (b–d) 2D DQ–SQ ^{1}H correlation spectra at 18.8 T and ν_R = 23.6 kHz. Three different homonuclear DQ recoupling sequences were compared, (b) BABA-1 with $\nu_{1\pi}$ = 91 kHz and τ = 42.4 μs, (c) BABA-2 with $\nu_{1\pi}$ = 91 kHz and τ = 84.8 μs, and (d) SPIP (Fig. 1e) with $\nu_{1\pi}$ = 91 kHz, ν_{1SL} = 59 kHz and τ = 169.5 μs. Each recoupling sequence employed experimentally optimized excitation and reconversion intervals, τ, and nutation frequencies. Each spectrum was acquired with 80 scans and a recycle delay of 2 s, leading to an acquisition time of 3.5 h for each spectrum.

one observes that BABA-1 is the most sensitive method to offsets, as F2 regions around −4 and +7 kHz are quite attenuated. BABA-2 also presents this problem at F2 ≈ −4 kHz (Fig. 8c), but moreover its on-resonance sensitivity is decreased by a factor of c.a. 3 with respect to that provided by BABA-1. This signal decrease is partly due to an increase of T_2' losses as the recoupling time of BABA-2 ($\tau = 2T_R$ = 84.8 μs) is twice longer than that of BABA-1. The SPIP spectrum (Fig. 8d) shows an on-resonance signal intensity comparable to that of BABA-1, but without any offset attenuation. These results are completely in agreement with previous simulations. As a result, the number of correlations revealed by the DQ–SQ experiment is small in the case of BABA-2 (5 cross- and 2 auto-peaks), moderate with BABA-1 (7 cross- and 3 auto-peaks) and large with SPIP (10 cross- and 3 auto-peaks), which allows revealing long distance correlations. The SPIP spectrum is similar to that published by Madhu and co-workers [9], who used the $C9_1^4$ DQ–SQ sequence, but it reveals more correlations (13 instead of 8) despite the fact that a PMLG decoupling method was used along F1 and F2 in ref [9], which increased the S/N ratio. Obviously, our spectra would have been quite improved by also using an homonuclear decoupling along F1 and F2 [32–34].

We have recorded several ^{31}P DQ–SQ spectra (not shown) on a phosphate sample which presents two phosphorous species, both submitted to a very large CSA of approximately 200 ppm. The BABA spectra recorded at 9.4 T with ν_R = 32 kHz, gave a poor S/N ratio, as opposed to those recorded with SPIP. The BABA spectra recorded at 18.8 T with ν_R = 20 kHz, gave no signal at all, and the efficiency observed on the SPIP spectra was not as good as that observed at 9.4 T. However, when taking off the spin-lock part of the sequence in Fig. 1e, the efficiency increased to c.a. 15%. The loss of efficiency observed with the initial SPIP sequence is related to the fact the rf-amplitude of the spin-lock parts was too small ($\nu_{1SL} \leqslant$ 100 kHz) to spin-lock efficiently such a large CSA (≈60 kHz at 18.8 T) [35].

At last, we show (Fig. 9) the SPIP DQ–SQ spectrum of NaH_2PO_4 recorded at 9.4T with Smooth Amplitude Modulation (SAM) homonuclear decoupling along F1 and F2 [34]. There are four different proton species in this sample [36], but two of them (H_3 and H_4) have very close chemical shifts [37]. All peaks are resolved in the 2D spectrum, and even on the 1D projections, and all diagonal and cross-peaks can be observed in this figure.

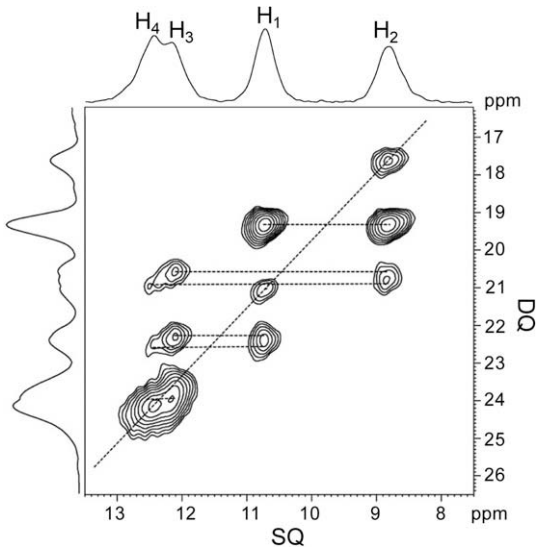

Fig. 9. 2D DQ–SQ ^{1}H correlation spectrum of NaH_2PO_4 recorded at 9.4 T and ν_R = 31.7 kHz using SPIP recoupling sequence. The excitation and reconversion intervals were τ = 504 μs and the rf nutation frequencies were $\nu_{1\pi}$ = 68 kHz and ν_{1SL} = 60 kHz. $SAM_{3.5}$ homonuclear decoupling sequence [34] was applied during t_1 and t_2 with maximal rf nutation frequency, ν_{1peak} = 121 kHz. The spectrum was acquired with 64 scans and a recycling delay of 1.5 s and the acquisition time was 5.4 h.

4. Conclusion

We have developed a new simple pulse sequence, christened SPIP, based on the rotor-synchronized $R2_2^1$ sequence. We have demonstrated that SPIP can be applied at fast (ν_R = 31.7 kHz here) spinning speeds. Although this method may experience relaxation decay during long recoupling periods, it provides a very broad band and efficient DQ homonuclear dipolar recoupling method and it is thus more appropriate in high magnetic fields than BABA sequences. The rf-amplitudes of the π pulse and spin-lock parts are moderate and do not have to fulfill stringent conditions. Therefore, the method is very robust and it does not require time-consuming optimization. SPIP recoupling may thus perform much better than BABA-1 and BABA-2 in protonated samples, such as proteins.

When the spinning speed is smaller than twice the frequency range of chemical shifts, folding of the resonances occurs along F_1. This may be avoided by introducing a π pulse in between the excitation and reconversion periods [26]. The position of this π pulse during the t_1 evolution time allows an easy scaling of all interactions in the indirect 2Q dimension, thus avoiding any possible folding.

Presently, the main limitation of all homonuclear dipolar methods is related to the dipolar truncation. This means that long-range correlations between two nuclei are not visible when one of these is also involved in a short-range correlation with a third-nucleus. A second limitation of these dipolar-based through-space methods is that unambiguous connectivity information can not strictly be ensured, as opposed to through-bond *J*-based methods. However, it is well-known that by a proper choice of a short dipolar recoupling time one may obtain the same results as with through-bond methods, at the expanse of the S/N ratio.

Acknowledgments

Authors are grateful for funding provided by Region Nord/Pas de Calais, Europe (FEDER), CNRS, French Minister of Science, FR-3050, USTL, ENSCL, Bruker BIOSPIN, and ANR Contract No. NT05-2-41632. They thank Dr. Fabian Aussenac for lending them its probe for the 400 MHz spectrometer.

References

[1] B.H. Meier, W.L. Earl, Excitation of multiple quantum transitions under magic angle conditions: adamantane, J. Chem. Phys. 85 (1986) 4905–4911.
[2] B.H. Meier, W.L. Earl, Double-quantum filter for rotating solids, J. Am. Chem. Soc. 109 (1987) 7937–7941.
[3] R. Tycko, G. Dabbagh, Measurement of nuclear magnetic dipole–dipole couplings in magic angle spinning NMR, Chem. Phys. Lett. 173 (1990) 461–465.
[4] R. Tycko, G. Dabbagh, Double-quantum filtering in magic-angle-spinning NMR spectroscopy: an approach to spectral simplification and molecular structure determination, J. Am. Chem. Soc. 113 (1991) 9444–9448.
[5] Y.K. Lee, N.D. Kurur, M. Helme, O.G. Johannessen, N.C. Nielsen, M.H. Levitt, Efficient dipolar recoupling in the NMR of rotating solids. A sevenfold symmetric radiofrequency pulse sequence, Chem. Phys. Lett. 242 (1995) 304–309.
[6] S.P. Brown, I. Schnell, J.D. Brand, K. Müllen, H.W. Spiess, The competing effects of π–π packing and hydrogen bonding in a hexabenzocoronene carboxylic acid derivative: a ^{1}H solid-state MAS NMR investigation, Phys. Chem. Chem. Phys. 2 (2000) 1735–1745.
[7] S. Pawsey, M. McCormick, S. De Paul, R. Graf, Y.S. Lee, L. Reven, H.W. Spiess, ^{1}H fast MAS NMR studies of hydrogen-bonding interactions in self-assembled monolayers, J. Am. Chem. Soc. 125 (2003) 4174–4184.
[8] S.P. Brown, Probing proton–proton proximities in the solid state, Prog. Nucl. Magn. Reson. Spectrosc. 50 (2007) 199–251.
[9] P.K. Madhu, E. Vinogradov, S. Vega, Multiple-pulse and magic-angle spinning aided double-quantum proton solid-state NMR spectroscopy, Chem. Phys. Lett. 394 (2004) 423–428.
[10] I. Schnell, Dipolar recoupling in fast MAS solid-state NMR spectroscopy, Prog. Nucl. Magn. Reson. Spectrosc. 45 (2004) 145–207.
[11] M. Edén, M.H. Levitt, Excitation of carbon-13 triple-quantum coherence in magic-angle spinning NMR, Chem. Phys. Lett. 293 (1998) 173–179.
[12] M. Carravetta, M. Edén, O.G. Johannessen, H. Luthman, P.J.E. Verdegem, J. Lugtenburg, A. Sebald, M.H. Levitt, Multiple-quantum ^{1}H MAS NMR studies of defect sites in as-made all-silica ZSM-12 zeolite, J. Am. Chem. Soc. 122 (2000) 6659–6663.
[13] X. Feng, Y.K. Lee, D. Sandström, M. Eden, H. Maisel, A. Sebald, M.H. Levitt, Direct determination of a molecular torsional angle by solid-state NMR, Chem. Phys. Lett. 257 (1996) 314–320.
[14] W. Sommer, D.E. Demco, S. Hafner, H.W. Spiess, Rotation-synchronized homonuclear dipolar decoupling, J. Magn. Reson. A 116 (1995) 36–45.
[15] M. Feike, D.E. Demco, R. Graf, J. Gottwald, S. Hafner, H.W. Spiess, Broadband multiple-quantum NMR spectroscopy, J. Magn. Reson. A. 122 (1996) 214–221.
[16] A. Brinkmann, M.H. Levitt, Symmetry principles in the nuclear magnetic resonance of spinning solids: heteronuclear recoupling by generalized Hartmann-Hahn sequences, J. Chem. Phys. 115 (2001) 357–384.
[17] M.H. Levitt, Encyclopedia of Nuclear Magnetic Resonance, Wiley, Chichester, 2002. pp. 165–196.
[18] S. Li, A. Zheng, Y. Su, H. Zhang, L. Chen, J. Yang, C. Ye, F. Deng, Brϕnsted/lewis acid synergy in dealuminated HY zeolite: a combined solid-state NMR and theoretical calculation study, J. Am. Chem. Soc. 129 (2007) 11161–11171.
[19] S.P. Brown, A. Lesage, B. Elena, L. Emsley, Probing proton–proton proximities in the solid-state: high-resolution two-dimensional ^{1}H–^{1}H double-quantum CRAMPS NMR spectroscopy, J. Am. Chem. Soc. 126 (2004) 13230–13231.
[20] M. Carravetta, Y. Murata, M. Murata, L. Heinmaa, R. Stern, A. Tontcheva, A. Samoson, Y. Rubin, K. Komatsu, M.H. Levitt, Solid-state NMR spectroscopy of molecular hydrogen trapped inside an open-cage Fullerene, J. Am. Chem. Soc. 126 (2004) 4092–4093.
[21] M. Carravetta, A. Danquigny, S. Mamone, F. Cuda, O.G. Johannessen, I. Heinmaa, K. Panesar, R. Stern, M.C. Grossel, A.J. Horsewill, A. Samoson, M. Murata, K. Komatsu, M.H. Levitt, Solid-state NMR of endohedral hydrogen-fullerene complexes, Phys. Chem. Chem. Phys. 9 (2007) 4879–4894.
[22] R. Graf, D.E. Demco, J. Gottwald, S. Hafner, H.W. Spiess, Dipolar couplings and internuclear distances by double-quantum nuclear magnetic resonance spectroscopy of solids, J. Chem. Phys. 106 (1997) 885–895.
[23] M. Eden, D. Zhou, J. Yu, Improved double-quantum NMR correlation spectroscopy of dipolar-coupled quadrupolar spins, Chem. Phys. Lett. 431 (2006) 397–403.
[24] A. Brinkmann, M. Eden, Second order average Hamiltonian theory of symmetry-based pulse schemes in the nuclear magnetic resonance of rotating solids: application to triple-quantum dipolar recoupling, J. Chem. Phys. 120 (2004) 11726.
[25] N.C. Nielsen, H. Bildsoe, H.J. Jakobsen, M.H. Levitt, Double-quantum homonuclear rotary resonance. efficient dipolar recovery in magic-angle spinning nuclear magnetic resonance, J. Chem. Phys. 101 (1994) 1805–1812.
[26] G. Mali, G. Fink, F. Taulelle, Double-quantum homonuclear correlation magic angle spinning nuclear magnetic resonance spectroscopy of dipolar-coupled quadrupolar nuclei, J. Chem. Phys. 120 (2004) 2835–2845.
[27] M. Carravetta, M. Eden, O.G. Johannessen, H. Luthman, P.J.E. Verdegem, J. Lugtenburg, A. Sebald, M.H. Levitt, Estimation of carbon–carbon bond lengths and medium-range internuclear distances by solid-state nuclear magnetic resonance, J. Am. Chem. Soc. 123 (2001) 10628–10638.

[28] J. Schmedt, Auf der Günne, Distance measurements in spin-1/2 systems by ^{13}C and ^{31}P solid-state NMR in dense dipolar networks, J. Magn. Reson. 165 (2003) 18–32.
[29] M. Bak, J.T. Rasmussen, N.C. Nielsen, SIMPSON: a general simulation program for solid-state NMR spectroscopy, J. Magn. Reson. 147 (2000) 296–330.
[30] M. Bak, N.C. Nielsen, REPULSION: a novel approach to efficient powder averaging in solid-state NMR, J. Magn. Reson. 125 (1997) 132–139.
[31] P.E. Kristiansen, M. Carravetta, J.D. van Beek, W.C. Lai, M.H. Levitt, Theory and applications of supercycled symmetry-based recoupling sequences in solid-state NMR, J. Chem. Phys. 12 (2006) 234510–234519.
[32] M. Leskes, P.K. Madhu, S. Vega, Supercycled homonuclear dipolar decoupling in solid-state NMR: toward cleaner ^{1}H spectrum and higher spinning rates, J. Chem. Phys. 128 (2008) 52309.
[33] B. Elena, G. de Paepe, L. Emsley, Direct spectral optimisation of proton–proton homonuclear dipolar decoupling in solid-state NMR, Chem. Phys. Lett. 398 (2004) 532–538.
[34] J.P. Amoureux, B. Hu, J. Trebosc, Enhanced resolution in proton solid-state NMR with very-fast MAS experiments, J. Magn. Reson. 193 (2008) 305–307.
[35] L. Delevoye, B. Hu, O. Lafon, J. Trebosc, J.P. Amoureux, submitted for publication
[36] R.N.P. Choudhary, R.J. Nelmes, K.D. Rouse, A room temperature neutron diffraction study of NaH_2PO_4, Chem. Phys. Lett. 78 (1981) 102–105.
[37] J. Rocha, J.P. Amoureux, ^{1}H-^{1}H double-quantum CRAMPS NMR at very-fast MAS (V_R = 35 kHz): a resolution enhancement method to probe ^{1}H-^{1}H proximities in solids, J. Magn. Reson 196 (2009) 89–91.